THREE-DIMENSIONAL STANDING WAVES ON AN OBLIQUELY FLOWING FILM

S. V. Alekseenko and S. I. Shtork

UDC 532.62+532.592

Waves which are almost always present on the surface of films flowing down an inclined surface have a strong effect on heat and mass transfer processes in the film [1, 2]. All of the existing studies of wavy fluid films have dealt with traveling waves occurring as a result of natural instability of the film flow or the superposition of artificial perturbations. However, standing as well as travelling waves exist on the film, the former being the result of local perturbations on the bottom or side walls of the channel. A complex system of standing waves develops when artificial wall roughness is employed in order to intensify heat transfer in films [3].

One feature of standing waves formed by localized perturbations is their three-dimensional character. The waves are horseshoe-shaped and correspond outwardly to single three-dimensional travelling waves (Fig. 1). Serious mathematical difficulties are encountered in any theoretical description of three-dimensional wave motion. No fewer problems arise in the experimental study of travelling three-dimensional waves due to their explicit transience and strong interaction with one another. Standing three-dimensional waves, in contrast to travelling waves, are convenient objects for detailed experimental study and for checking two- and three-dimensional wave theories.

Here, we experimentally and theoretically investigate the dispersion and form of the crests of three-dimensional standing waves on an obliquely flowing film of a viscous fluid within a broad range of angles of inclination and fluid discharges and properties.

Experimental Procedure. The tests were conducted on an experimental unit consisting of a working section — a trough — and a receiver tank, centrifugal pump, rotameters, and control valves. The trough was a smooth organic-glass plate 150 mm wide and 1000 mm long. The film of fluid flowed over the surface of this plate. The fluid reached the surface of the plate by being poured over its rounded edge from a distributing tank attached to the trough. Flowing from the trough, the fluid was collected in the receiver tank. The receiver tank was also attached to the chute. The film flow was bounded laterally by metal walls with a ground surface.

The trough was set on a post which made it possible to finely regulate its inclination in two planes. The angle of inclination of the trough to the horizontal was changed from 75 to 2.75° in the tests. The accuracy of measurement of the angle of inclination was 0.25°.

The thickness of the film in the wave-free zone was measured by the contact method using a needle attached to a dial gage with graduations of 0.01 mm. Fluid discharge was determined from the readings of RS-5 rotameters. Fluid temperature was recorded by a mercury thermometer with graduations of 0.1°C. The uniformity of wetting of the trough surface was monitored visually from the symmetry of the wave pattern and from values of film thickness at different points of the trough.

Stationary standing waves were created in the smooth zone of the trough by having the sharp tip of the needle touch the surface of the film. The characteristics of the waves (form of crests and wavelength) were determined from photographs made on the side of the wetted surface of the trough. Typical photographs of the standing waves are shown in Fig. 1a and b. The wavelength was measured only in the direction of the flow. The accuracy of these measurements was within the range 2-7%. It was found that the wavelength and crest shape are independent of the depth of submersion of the needle.

As the working fluid we used distilled water and solutions of ethyl alcohol and glycerin. The physical properties of the main solutions and the ranges of Reynolds numbers Re and angles

Krasnoyarsk. Translated from Zhurnal Prikladnoi Mekhaniki i Tekhnicheskoi Fiziki, No. 4, pp. 157-164, July-August, 1987. Original article submitted August 5, 1986.

 0021-8944/87/2804-0618$12.50

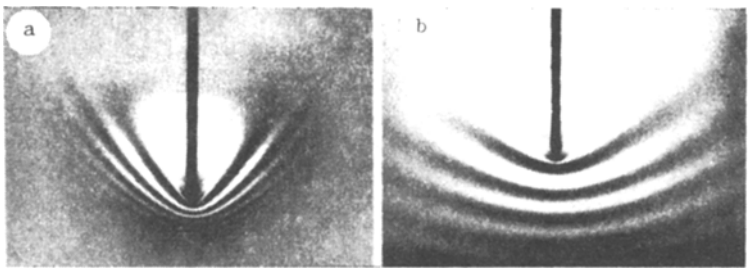

Fig. 1

TABLE 1

Fluid	$\nu \cdot 10^6$, m^2/sec	$\sigma/\rho \cdot 10^6$, m^3/sec^2	$Fi^{1/11}$	Re	θ, deg
Water	0,9	71,8	9,51	600 ... 90	75 ... 2,75
Aqueous solution of glycerin	2,0	63,4	6,9	350 ... 60	75 ... 5,25
Aqueous solution of ethanol	1,6	42,7	6,7	450 ... 75	75 ... 5,25

of trough inclination θ are shown in Table 1, where t is temperature, ν is viscosity, σ is surface tension, ρ is fluid density, $Fi = \sigma^3/\rho^3 g\nu^4$ is the film number, g is acceleration due to gravity, $Re = q/\nu$, and q is the discharge of the fluid.

Dispersion of the Standing Waves. Since the absolute phase velocity c = 0 for standing waves, by the dispersion we mean the dependence of the wavelength λ (or wave number k) on flow velocity. In analyzing data, it is convenient to use Re rather than flow velocity. The Nusselt relations (below) are valid for a smooth laminar steady-state flow

$$\mathrm{Re} = gh^3 \sin\theta/3\nu^2 = q/\nu, \quad u_S = gh^2 \sin\theta/2\nu,$$

where u_S is the velocity on the surface of the film; h is the thickness of the film. The dimensionless wave number is determined as $\bar{k} = kh = 2\pi h/\lambda$.

Our experiment showed that there are both short ($\bar{k} \gg 1$) and long ($\bar{k} < 1$) standing waves on the film surface. Almost all existing theories of wavy fluid films are based on a long-wave approximation, but these theories are unsuitable for describing standing waves in the great majority of cases because there are no solutions c = 0.

A universal two-wave model equation for long waves on an obliquely flowing film was derived in [4]. It describes different types of waves, including standing waves. It was used in [4] to obtain the dispersion relation

$$(\bar{k}\,\mathrm{Re})^2 = \frac{B}{6}[\bar{c}^2 - 2{,}4\bar{c} + 1{,}2 - A]\left\{1 \pm \left[1 + \frac{27(\bar{c}-3)(\bar{c}+0{,}6)}{B(\bar{c}^2 - 2{,}4\bar{c} + 1{,}2 - A)^2(\bar{c}-1{,}2)^2}\right]^{1/2}\right\}. \tag{1}$$

Here, the dimensionless phase velocity $\bar{c} = c/u_0$; the mean velocity $u_0 = gh^2 \sin\theta/3\nu$; $A = 3 \cot\theta/\mathrm{Re}$; $B = \mathrm{Re}^3 \sin\theta/\mathrm{We}$; the Weber number $\mathrm{We} = \sigma/\rho g h^2$.

Equation (1) has two pairs of nonintersecting roots, only one of which was analyzed in [4]. The complete dispersion curves are shown in Fig. 2 for Re = 50, θ = 75°, $Fi^{1/11} = 9.51$ (water). The two branches of the dispersion curve are symmetrical relative to the axis $\bar{c} = 1.2$. It follows from the complete dispersion relations [4] that the waves grow exponentially over time at phase velocities $1.2 < \bar{c} < 3$ and decay exponentially at $\bar{c} > 3$ and $\bar{c} < 1.2$. Neutral waves exist at $\bar{c} = 3$.

The linear asymptotes of the dispersion curves at high $\bar{k}$ are described by the relation

$$\bar{c} = 1.2 \pm \bar{k}(3\,\mathrm{We}\,\mathrm{Re}\sin\theta)^{1/2}$$

or, in dimensional form

$$c = 1.2u_0 \pm \frac{2\pi}{\lambda}\sqrt{\frac{\sigma h}{\rho}}. \tag{2}$$

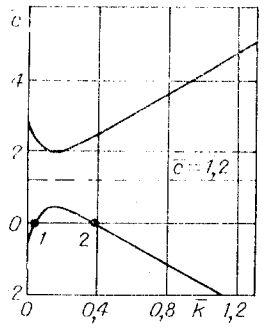

Fig. 2

This is the dispersion law for capillary waves on shallow water. The term $1.2u_0$ reflects the contribution of the mean flow.

Assuming $\bar{c} = 0$, we use (1) to obtain the dispersion relation for standing waves

$$\bar{k} = \frac{1}{\mathrm{Re}}\left\{\frac{B}{6}(1{,}2 - A)\left[1 \pm \sqrt{1 - \frac{27}{0{,}8B(1{,}2 - A)^2}}\right]\right\}^{1/2}, \tag{3}$$

having two roots $\bar{k}_1$ and $\bar{k}_2$, corresponding to points 1 and 2 in Fig. 2. At point 1, the group velocity $c_g = c + \bar{k}dc/d\bar{k} > c$, since $dc/d\bar{k} > 0$. Thus, in accordance with the theory of dispersive waves, waves with $\bar{k}_1$ will be formed downstream of an obstacle.

At point 2, $\bar{c}_g < \bar{c}$. Thus, perturbations with $\bar{k}_2$ develop ahead of the obstacle.

Equation (3) can be rewritten in more compact form

$$\bar{k}_S = \left[\frac{S}{6}\left(1 \pm \sqrt{1 - \frac{33.75}{S^2}}\right)\right]^{1/2}, \tag{4}$$

where now the dimensionless wave number $\bar{k}_S = \bar{k}(\mathrm{Re\ Fi}/9 \sin\theta)^{1/12}$ is a function of only one parameter $S = (1.2 - 3 \cot\theta/\mathrm{Re})(\mathrm{Re}^3 \sin\theta/\mathrm{We})^{1/2}$. It follows from Eq. (4) that there exists a critical number (or a critical film thickness)

$$S^* = \sqrt{33.75}, \tag{5}$$

and standing waves cannot exist on the film surface at values lower than this number. This condition is analogous to the existence of a minimum velocity for capillary–gravitational waves on the surface of an ideal fluid [5, 6]. For example, $\mathrm{Re}^* = 19$ for water at $\theta = 75°$ and $\mathrm{Re}^* = 63$ at 2.75°. It should be noted that the critical Re^* for standing waves is markedly different from the critical Re for the formation of travelling waves, which is equal to $\cot\theta$ [1].

In the tests we conducted, waves were seen only under the conditions $\mathrm{Re} \gg 3 \cot\theta$, $S \gg S^*$. Then Eq. (3) takes the simpler form

$$\bar{k} = 0.91(\mathrm{Re}/F)^{5/6} \tag{6}$$

or

$$\lambda = \frac{6\pi\nu}{g \sin\theta}\sqrt{\frac{\sigma}{1.2\rho h^3}},$$

where the complex $F = (\mathrm{Fi} \sin\theta)^{1/5} = (\sigma^3 \rho^3 g \nu^4 \sin\theta)^{1/5}$.

Equation (6) is valid at $h/\lambda \ll 1$. However, experience shows that short standing waves with $h/\lambda \gg 1$ also exist on the film. Since short, low-amplitude surface waves are nearly "insensitive" to the wall and, thus, to viscosity, then it is natural to attempt to describe such waves by means of the theory of an ideal fluid. We have the following dispersion law [5] for capillary waves on deep water

$$c = \sqrt{\sigma k/\rho}. \tag{7}$$

Equating the phase velocity of the waves to the surface velocity of the fluid u_S, we find

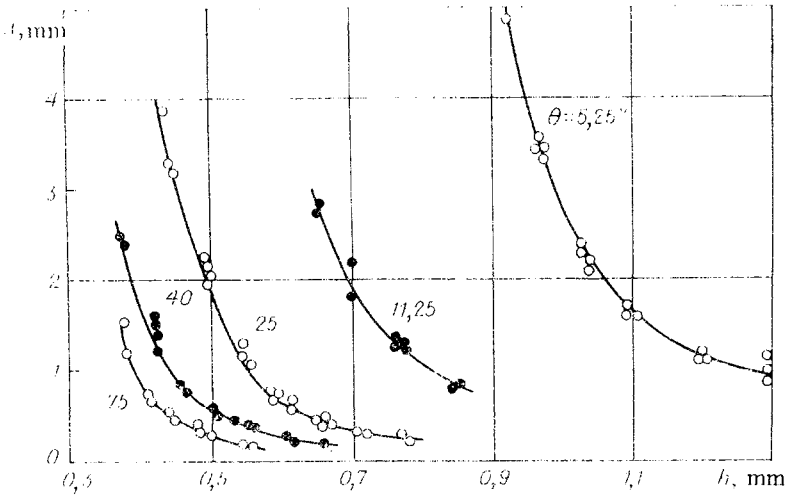

Fig. 3

$$\lambda \quad \frac{\sigma}{\rho}\frac{8\pi\nu^3}{g^2\sin^2\theta}\frac{1}{h^4}$$

or, in dimensionless form

$$\bar{k} \quad 1{,}56(\mathrm{Re}/F)^{5/3}. \tag{8}$$

As in the case of long waves on a viscous fluid, the wave number depends only on one complex Re/F.

The dispersion law $c = k\sqrt{\sigma h/\rho}$ for capillary waves on shallow water [5] leads us to the formula

$$\bar{k} = 1{,}25(\mathrm{Re}/F)^{5/6}, \tag{9}$$

for which it is useful to make a comparison with Eq. (6). It is evident that, other conditions being equal, the effect of viscosity is appreciable only in the numerical coefficient.

Figure 3 shows experimentally measured values of the length of standing waves along the direction of film flow. Film thickness was determined from the theoretical Nusselt formula $h = (3q\nu/g \sin\theta)^{1/3}$. The need to use the theoretical thickness instead of the measured thickness is due to the fact that the smooth zone is almost always located within the initial section of the film – where the film thickness changes with distance (and is always greater than the theoretical value for the given type of inlet apparatus). Thus, all of the measurements were made at the end of the smooth zone near the wave-formation line, where deviations of the measured thickness from the theoretical value were minimal and did not exceed 10%.

The test data was obtained under laminar flow conditions, i.e., at $\mathrm{Re} \lesssim 400$-600. The minimum values of Re at which we could still observe standing waves was limited either by the critical values which follows from (5) or by the existence of travelling waves – which at small Re cover nearly the entire surface of the film. It should be noted that the actual values of Re* were considerably greater than the theoretical values. As can be seen from Fig. 3, wavelength decreases with an increase in film thickness. Given a film thickness, an increase in the angle of inclination also leads to a reduction in wavelength.

Figure 4 shows experimental data generalized in the dimensionless coordinates $[\bar{k}, \mathrm{Re}/F]$, which follow from the theoretical examination. The test points 1-3 pertain, respectively, to the water and solutions of glycerin and alcohol. The properties of these solutions are shown in Table 1 along with other information. The effect of Re, the angle θ, and the distance x is not shown on the graph, since all of the points are generalized within the range of measurement accuracy in the coordinates we used.

At $\bar{k} \gtrsim 5$, the experimental points are located along relation I, which was obtained in a short-wave approximation for waves on the surface of an ideal fluid [Eq. (8)]. The systematic displacement of points downward from the theoretical relation is evidently due to the fact that the flow has not completely stabilized. In fact, with a stabilized flow, the surface velocity is somewhat higher and the length of the standing waves is somewhat smaller.

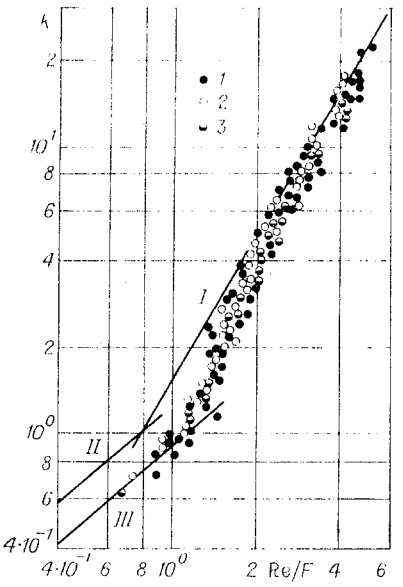

Fig. 4

On the whole, this led to an increase in the measured values of $\bar{k}$ and, thus, to an improvement in the correlation between the theory and experiment.

The experimental points begin to deviate from relation I at $\bar{k} < 5$, and at $\bar{k} \lesssim 1$ they already lie along line III, obtained for long waves on the surface of a viscous fluid [Eq. (6)]. The minimum values of $\bar{k}$ which were reliably measured in the experiment reached 0.6. For comparison, Fig. 4 shows curve II, constructed from Eq. (9) for an ideal fluid and passing 37% above line III.

Thus, at $\bar{k} \gtrsim 5$, the standing waves are described by the short-wave approximations of the theory of waves on the surface of an ideal fluid. At $1 \lesssim \bar{k} \lesssim 5$, there is a transition from short to long waves accompanied by an increase in the effect of viscosity. At $0.6 \lesssim \bar{k} \lesssim 1$, the theory of long waves on the surface of a flowing viscous film is valid. At $\bar{k} < 0.6$, no standing waves are seen.

Form of the Crests of Three-Dimensional Standing Waves. A simple approach was proposed in [5] for constructing the form of the crests of dispersive waves generated by a moving source. It was shown that in the case of a constant source velocity, the form of the crests is determined only by the ratio of the group velocity to the phase velocity. In particular, this approach can be used in theories of ship waves and waves on the surface of a layer of ideal fluid [5, 6].

Different dispersion laws [see Eqs. (1) and (7), as well as Fig. 2] exist for an obliquely-flowing viscous film, depending on the range of wave numbers. We will therefore use Lighthill's approach for a fairly general case, when the dispersion relations are approximated by a power law

$$c = c_1 k^{\gamma - 1},$$

where $\gamma < 1$; c_1 is a constant. The group $c_g = c + kdc/dk = \gamma c$, i.e., γ is the ratio of the group velocity to the phase velocity. Thus, $\gamma = 3/2$ for dispersion (7), $\gamma = 2$ for capillary waves on shallow water, and $\gamma = 1$ for nondispersive waves.

The construction of the crests of three-dimensional waves is shown in Fig. 5. Let the source of the perturbation move at a velocity u in the direction of negative values of x and let it be located at the origin at the moment of time τ. We will find the position of waves which are stationary relative to the source and are generated at the moment of time $\tau = 0$ for the moment when the source is located at the point (X, 0). We write the condition of stationariness of the wave front, moving in the direction φ, in the form $c = u \cos \varphi$. Then a wave propagating at the angle φ will travel the distance $CB' = u \cos \varphi \tau$. However, in reality, it follows from the theory of dispersive waves that this wave will be seen at the distance $CB = c_g \tau = \gamma c \tau = \gamma u \cos \varepsilon \tau$, i.e., γ times farther. Analogously, $CA = \gamma u \tau$. It follows from the last two relations that $BC = AC \cos \varphi$, so that the angle ABC is a right angle. Thus, the locus B is a circle.

Let us determine the form of the crest. The generatrix of the crest is perpendicular to the direction of propagation of the wave CB. We use geometric constructions to find the coordinates of the point B:

$$x = \gamma X \sin 2\varphi / 2, \quad y = X(1 - \gamma \cos^2 \varphi). \tag{10}$$

The angle of inclination of the wave front at point B relative to the x axis is determined by the expression

$$dy/dx = \operatorname{ctg} \varphi. \tag{11}$$

Inserting (10) into (11) and solving the resulting ordinary differential equation, we obtain $X = b(\cos \varphi)^{\gamma/(\gamma-1)}$, where b is the constant of integration. Excluding X from (10), we obtain the equations

$$y = \gamma b \sin \varphi (\cos \varphi)^{1/(\gamma-1)}, \quad x = b(1 - \gamma \cos^2 \varphi)(\cos \varphi)^{\gamma/(\gamma-1)},$$

which in parametric form describe the shape of the crests of the standing waves. The constant b remains indeterminate within the framework of the linear theory.

It is convenient to use dimensionless equations. To do this, we introduce the dimensionless coordinates $\bar{x} = x/a$, $\bar{y} = y/a$, where $a = -x|_{\varphi=0} = |1 - \gamma|$ is the distance from the source to the crest of the wave along the y axis. To simplify the notation, we put $\cos^2 \varphi \equiv \alpha$. Then we finally have

$$\bar{y} = \frac{\gamma}{\gamma - 1} \frac{\sqrt{1 - \alpha}}{\alpha^{1/2(\gamma-1)}}; \tag{12}$$

$$\bar{x} = \frac{1 - \gamma\alpha}{\gamma - 1} \frac{1}{\alpha^{\gamma/2(\gamma-1)}}. \tag{13}$$

In the case of long capillary waves ($\gamma = 2$), system (12)-(13) reduces to the single formula

$$\bar{x} = -1 + \bar{y}^2/4 \tag{14}$$

which gives a wave crest of parabolic form. At $\bar{x} = 0$, $\bar{y} = \bar{y}_0 = 2$ ($\bar{y}_0$ is a characteristic of the crest shape).

For short capillary waves, $\gamma = 3/2$, and Eqs. (12) and (13) take the form

$$\bar{x} = (2 - 3\alpha)/\alpha^{3/2}; \tag{15}$$

$$\bar{y} = 3\sqrt{1 - \alpha}/\alpha. \tag{16}$$

The form of the crest constructed from (15) and (16) is shown in Fig. 6 (line 1). At $\bar{y} \to \infty$ in the asymptote, we obtain the power law $\bar{x} = 2(\bar{y}/3)^{3/2}$.

Table 2 shows values of the crest shape characteristics – the distance $\bar{y}_0$ and the angle ψ represented in Fig. 6 – as a function of the dispersion law.

The three-dimensional standing waves and the travelling waves seen in the experiment were analyzed as follows. First we chose the presumed dispersion law. We then used the angle ψ to determine the position of the coordinate origin (the position of the source) for a specific crest, as shown in Fig. 6. The distance OA served as the characteristic scale in converting the coordinates of the crest to dimensionless form. For naturally formed travelling waves, the origin should be regarded as the location of an equivalent source. The same can be said in the case of analysis of standing waves with an arbitrarily chosen dispersion law, when the position of the actual source and the calculated coordinate origin do not coincide.

In coordinates chosen for a dispersion law with $\gamma = 3/2$, Fig. 6 shows experimental data for short three-dimensional standing waves ($\bar{k} \gtrsim 5$) at different Re, fluid properties, and angles of trough inclination θ. The theoretical form of the crest (line 1) was constructed from Eqs. (15) and (16). Each specific crest was represented by 8 points. We thus analyzed more than 100 crests. This included different crests from one source (such as all of the crests depicted in Fig. 1, a and b). Different points in Fig. 6 correspond to different

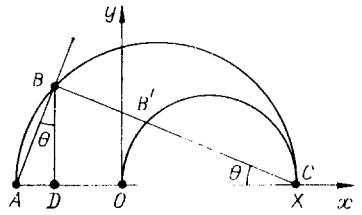

Fig. 5

TABLE 2

ν	$\bar{y}_0$	ψ
4	1,45	55°30′
3	1,61	58°11′
2	2,00	63°26′
3/2	2,6	68°57′
4/3	3,08	72°

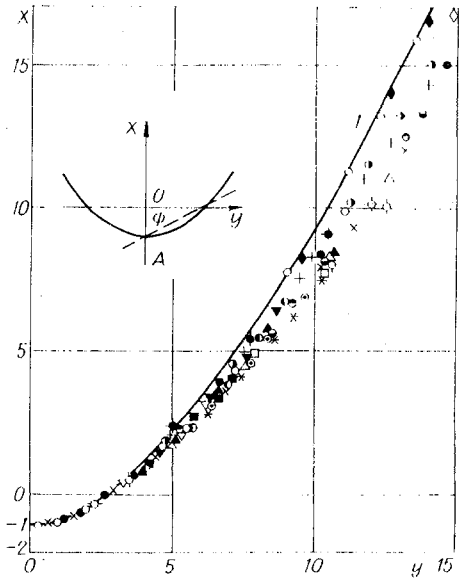

Fig. 6

crests under different conditions. However, these conditions are not manifest on the graph, since, within the statistical scatter, we found that Re, the fluid properties, the angle of inclination θ, and the serial number of the crest did not affect the analysis of the data in the above coordinates at $\bar{k} \geq 5$.

It follows from the graph that the deviation of the experimental points from the theoretical curve is 0-20%. The same data analyzed in the coordinates for a dispersion law with $\gamma = 2$ deviates considerably from the corresponding theoretical curve.

Long standing waves with the wave number $\bar{k} < 1.5$ were analyzed in the coordinates for dispersion laws with $\gamma = 2$ and 1.5. The data was readily generalized in dimensionless coordinates, but the experimental points again systematically deviated downward from the theoretical curve. One unexpected finding was that better agreement is obtained between the theory and experiment for long standing waves in the case of a dispersion law with $\gamma = 3/2$ (i.e., in the short-wave case).

A similar analysis was made of travelling three-dimensional waves, although in this instance it was difficult to expect good results in view of the transience and nonlinearity of travelling waves. Nevertheless, a satisfactory generalization and agreement between the theory and experiment were obtained (albeit with a large scatter of points) if we set $\gamma = 2.2$. It should be noted that this value is close to the value of γ for long capillary waves.

To adequately describe three-dimensional standing waves on a flowing viscous film, it is evidently necessary to examine the three-dimensional equations of motion in order to allow for the dependence of phase velocity not only on the wave number, but also on the direction of wave propagation.

LITERATURE CITED

1. S. V. Alekseenko, V. E. Nakoryakov, and B. G. Pokusaev, Waves on the Surface of a Vertically Flowing Film of Fluid, Preprint, ITF SO AN SSSR, Novosibirsk (1979), No. 36-79.
2. V. E. Nakoryakov, B. G. Pokusaev, and S. V. Alekseenko, "Effect of waves on the desorption of carbon dioxide on flowing liquid films," Teor. Osn. Khim. Tekhnol., 17, No. 3 (1983).
3. A. G. Sheinkman, E. F. Ratnikov, and S. E. Shcheklein, "Study of heat transfer on a fluid film turbulently flowing over a rough vertical surface," in: Nonlinear Waves Processes in Two-Dimensional Media [in Russian], ITF SO AN SSSR, Novosibirsk (1977).
4. V. E. Nakoryakov and S. V. Alekseenko, "Waves on an obliquely flowing fluid film," in: Wave Processes in Two-Dimensional Media [in Russian] ITF SO AN SSSR, Novosibirsk (1980).
5. J. Lighthill, Waves in Fluids, Cambridge Univ. Press (1979).
6. D. B. Witham, Linear and Nonlinear Waves [Russian translation], Mir, Moscow (1977).